Vortex state in a $Nd_{1.85}Ce_{0.15}CuO_{4-\delta}$ single crystal

A. A. Nugroho and I. M. Sutjahja
Van der Waals–Zeeman Instituut, Universiteit van Amsterdam, Valckenierstraat 65 1018 XE, Amsterdam, The Netherlands and Jurusan Fisika, Institut Teknologi Bandung, Jl Ganesha 10 Bandung 40132, Indonesia

M. O. Tjia
Jurusan Fisika, Institut Teknologi Bandung, Jl Ganesha 10 Bandung 40132, Indonesia

A. A. Menovsky, F. R. de Boer, and J. J. M. Franse
Van der Waals–Zeeman Instituut, Universiteit van Amsterdam, Valckenierstraat 65 1018 XE, Amsterdam, The Netherlands
(Received 18 May 1999)

Magnetization data of a $Nd_{1.85}Ce_{0.15}CuO_{4-\delta}$ single crystal prepared by the traveling solvent floating zone method reveal a feature showing a sharply defined temperature range for the occurrence of the second-peak effect. A vortex phase diagram derived from these data on the basis of some of the existing models displays a number of perceptible changes in the temperature dependencies of the penetration field H_p, the irrevesibility line H_{irr}, and the symmetry of the hysteresis loop, in conjunction with the observation of the peak effect. It is shown that effective penetration of the external magnetic field in the three-dimensional vortex regime is a prerequisite to the transition from its quasilattice to disordered glass vortex state associated with occurence of the peak effect. Comparison with previous results on a similar sample further indicates certain sample-dependent nature of the data. [S0163-1829(99)02345-0]

INTRODUCTION

Since its discovery in a single-crystalline $YBa_2Cu_3O_{7-\delta}$ (YBCO),[1] the second peak occurring at low field as an arrow head in the magnetization curve has now been observed in relatively clean single crystals of $Tl_2Ba_2CuO_6$ (TBCO),[2] $Bi_2Sr_2CaCu_2O_8$ (BSCCO),[3,4] $La_{2-x}Sr_xCuO_{4-\delta}$,[5] and $Nd_{1.85}Ce_{0.15}CuO_{4-\delta}$ (NCCO).[6] This anomalous effect has been extensively studied, and attributed to mechanisms varying from collective pinning,[7] surface barriers,[2,3,6] lattice matching between vortex and defect structure,[8] three-dimensional–two-dimensional (3D-2D) dimensional cross over,[9] crossover between elastic and plastic states[10] to crossover between quasilattice vortex glass and disordered vortex glass.[11–13] Some of these theoretical explanations stand up against the accumulating experimental data better than the others. None of them alone, however, provides a complete description of the effect. Even the more promising models are still subject to further experimental scrutiny. This is particularly true in view of growing experimental evidence on the one hand and the current shortage of high-quality experimental data available to date on the other. For instance, the fact that most of the available data are obtained by global measurements of the magnetization loop may somehow suppress the salient feature of a sharp transition in the peak effect. Furthermore, while generally reported with a clear onset temperature below T_c, most of the data fail to delineate the temperature range in which this remarkable effect persists. An exception to this has been reported on BSCCO (Refs. 14 and 15) for which a temperature range of 22 to 28 K was cited for the observation of peak effect. Added to these shortcomings are the nonuniform quality of samples studied so far. As a consequence, additional experimental data and related phenomenological analysis are needed before a comprehensive and definitive picture of the associated vortex phase diagram may emerge from these studies.

The relatively moderate anisotropy ($\gamma = 200$) (Ref. 16) and the low-T_c (T_c between 21 and 24 K) of NCCO offer a special advantage for the study of those putative transitional effects as the phenomena are expected to be relatively free from thermal complications and within easily accessible range of magnetic measurement. In this paper, we report the result of magnetic-hysteresis loop measurements on a high-quality $Nd_{1.85}Ce_{0.15}CuO_{4-\delta}$ single crystal. In contrast to the results reported by Andrade *et al.*,[17] a clearly reproducible peak effect is observed within a limited temperature range, showing a discernible sign of disappeareance of the arrow head at lower temperature in conjuction with a number of other effects. Analysis of these coincidental effects will be shown to suggest a relatively comprehensive picture of the vortex states covering the peak-effect region and its surrounding area in the H-T phase diagram.

EXPERIMENTS

The experiments were performed on a single crystal of $Nd_{1.85}Ce_{0.15}CuO_{4-\delta}$ grown by The traveling solvent floating zone (TSFZ) method using a four-mirror furnace from Crystal System Inc. The crystal with dimensions $\sim 1.5 \times 2.5 \times 0.01$ mm^3 and mass of 1.6 mg was obtained by cleaving the as-cut crystal along the ab plane in air. The as-grown crystal was not a superconductor. It became superconducting at $T_c \sim 21$ K (with $\Delta T_c \sim 1$ K) as shown in Fig. 1 after being annealed in flowing N_2 gas at 900 °C for 30 h and subsequently quenched to room temperature. The superconductivity can be easily removed by annealing the superconducting crystal at 900 °C in air. The elemental composition of the crystal was examined by means of electron micro-

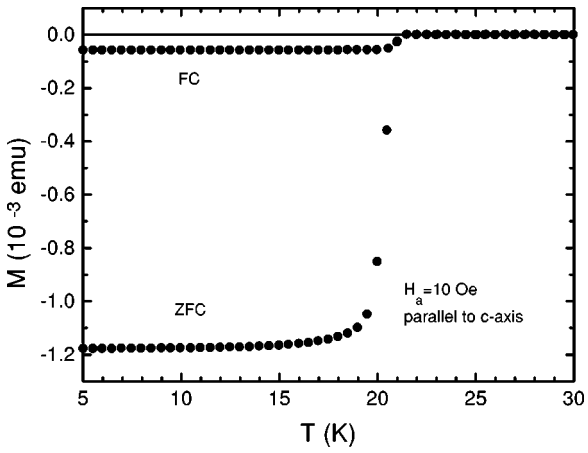

FIG. 1. Temperature dependence of the magnetization of $Nd_{1.85}Ce_{0.15}CuO_{4-\delta}$ with $T_c = 21$ K measured in an applied field of 10 Oe parallel to the c axis.

probe analysis (EPMA), and the result shows that the molar ratios are given by Nd:Ce:Cu:O=1.98:0.15:1:3.59, which is relatively rich in Nd.

Isothermal magnetic-hysteresis loops were measured with the magnetic field H applied parallel to the c axis of the crystal using a commercial Quantum Design MPMS-5 magnetometer. The measurements were carried out in the temperature range $5 \leqslant T \leqslant 20$ K, with field steps of $10 \leqslant H \leqslant 50$ Oe and $50 \leqslant H \leqslant 350$ Oe below and above the second peak, respectively. Each measurement was started after the sample was zero-field cooled to a predetermined temperature with the scan length set at 4 cm.

RESULTS AND DISCUSSION

Figures 2 –4 show the magnetic-hysteresis loops $M(H)$ in the low-field region with the penetration field H_p, onset field for the second peak H_{on}, the second peak H_{sp}, and the irrevesible field H_{irr} indicated on the curves. The curves exhibit the following features: (1) An onset temperature of the second peak at $T \sim 19.5$ K, which is very close to T_c, with $H_{on} \sim 100$ Oe, in reasonable agreement with an observation reported previously.[17,18] (2) A discernible disappearance of the second peak below about $T \sim 10$ K ($T/T_c < 0.5$), in clear contrast to results reported in Refs. 17 and 18. (3) An abrupt increase of the penetration field at about 10 K, where the second peak disappears. It must be stressed that in all high-T_c cases reported so far, the onset temperature of the peak effect generally lies far below T_c ($T/T_c < 0.5$). Additionally, the disappearance of the effect was not commonly reported, except in the case of a BSCCO crystal for which a temperature range between 22 and 28 K was cited for the observation of the effect.[14,15]

Following the scaling treatment introduced previously for

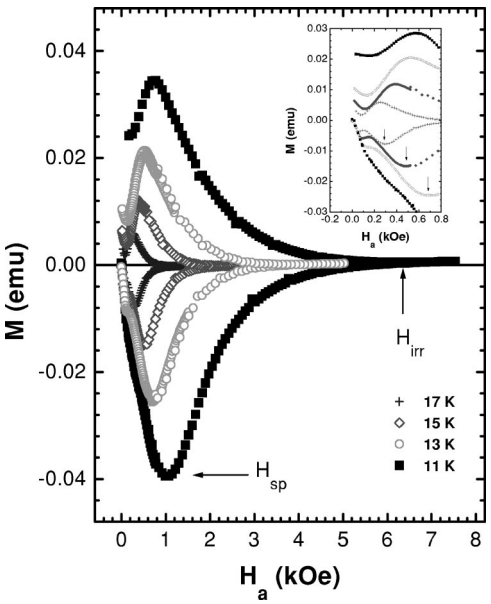

FIG. 3. Isothermal magnetic-hysteresis loops of a NCCO single crystal at various temperatures between 11 and 17 K. The positions of H_{sp} between 11 and 15 K are indicated in the inset.

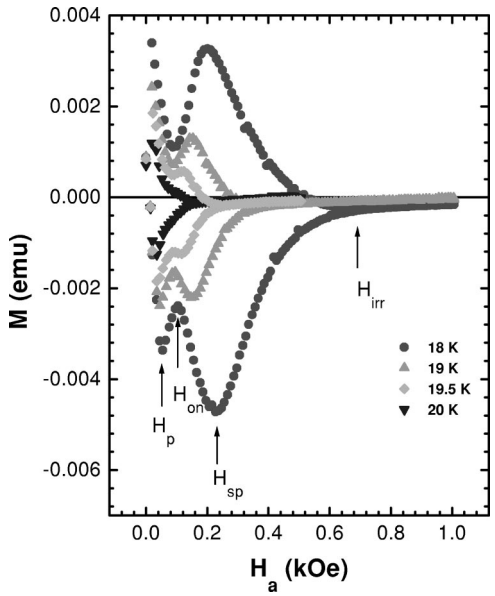

FIG. 2. Isothermal magnetic-hysteresis loops of a NCCO single crystal at various temperatures between 18 and 20 K.

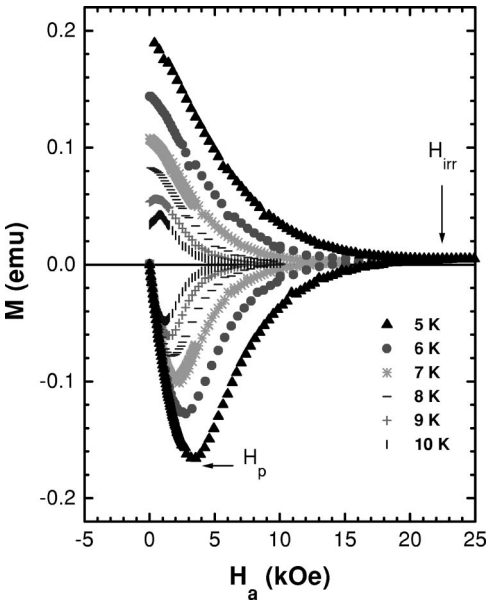

FIG. 4. Isothermal magnetic-hysteresis loops of a NCCO single crystal at various temperatures between 5 and 10 K.

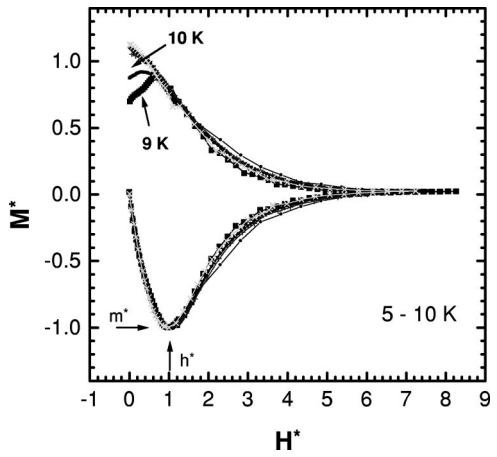

FIG. 5. Scaling of the isothermal magnetic-hysteresis loops with respect to magnetic moment (m^*) as well as magnetic field (h^*) at the first penetration point for low-temperature regime $5<T<10$ K. The lines are used for guiding the eye.

a BSCCO crystal,[19] the $M(H)$ curves at various temperatures presented in Figs. 2–4 are similarly treated here. For each curve, the field and moment are scaled with the magnetic moment (m^*) and the magnetic field (h^*) at the first penetration point indicated in the figure. The results are presented separately in Fig. 5 and Fig. 6 for different temperature ranges. Figure 5 shows the normalized magnetization curves at temperatures between 5 and 10 K, which are below the temperature range of the second peak. A remarkable scaling behavior is displayed over the entire range of the hysteresis loop for 5, 6, and 7 K. It is further observed that a distinct deviation from the scaling behavior begins to show up at 9 K, which is at about the lower end of the temperature range of the second peak. In this temperature range the scaling characteristic is almost completely lost; it is retained only in the very narrow region far below h^* as depicted in Fig. 6. Unfortunately, it is impossible to investigate the expected recovery of the scaling behavior at the high-temperature end of the peak effect ($T\sim 19.5$ K), as the interval between this temperature and the critical-transition temperature is simply too narrow to allow a meaningful comparison of distinctly different magnetization curves.

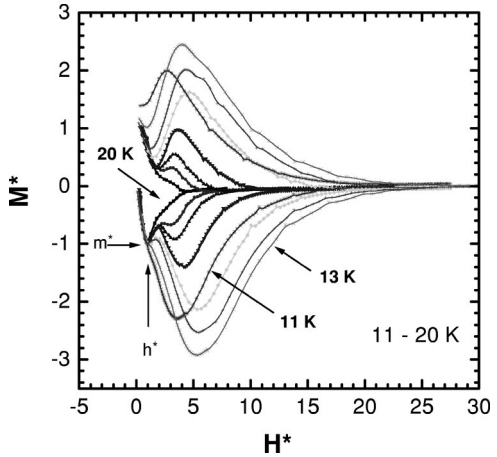

FIG. 6. Scaling of the isothermal magnetic-hysteresis loops with respect to magnetic moment (m^*) as well as magnetic field (h^*) at the first penetration point for high-temperature regime $11<T<20$ K. The lines are used for guiding the eye.

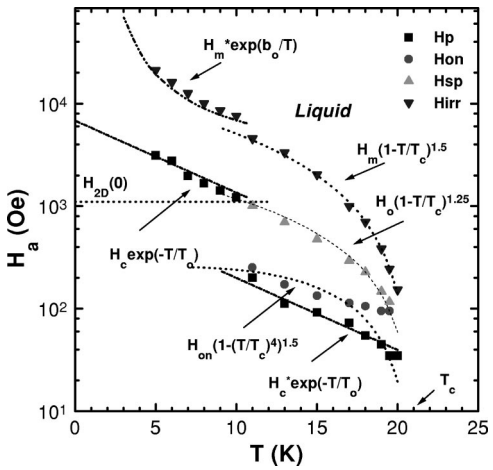

FIG. 7. H-T phase diagram for a NCCO single crystal with theoretical fits of the temperature dependencies of H_p, H_{on}, H_{sp}, and H_{irr}. See text for the discussion.

Another important aspect revealed by Fig. 5 is the onset and disappearance in the different temperature regions of the symmetry between the two branches of the hysteresis loop. It is apparent that a pronounced asymmetry features in the scaled data at temperatures below 10 K. To a lesser extent, a similar feature is also perceptible for the data at 20 K represented by the innermost curve in Fig. 6. On the other hand, a symmetrical shape of the hysteresis loops is consistently displayed in the figure for all curves with T lying within the temperature range of the peak effect. Similar behavior has previously been reported for a BSCCO.[14,15] It is important at this point to recall that the symmetrical shape of the hysteresis loop is supposed to indicate a dominant role of the bulk pinning mechanism, while the decrease of the symmetry is understood to signify the increasing role of the surface or the geometrical barriers in the pinning mechanism. Hence, it is natural to suggest on this general ground that the second-peak effect is expected to appear in a temperature and field regime where the bulk pinning effect is dominant and disappear outside this regime due to suppression of the pinning mechanism. This general picture appears to be well in line with the suggestion offered in Ref. 19. A more detailed description will emerge in the following discussion.

For the purpose of further analysis, the experimental M-H curves in Figs. 2–4 are converted to H-T semilogarithm plots in Fig. 7. This conversion is carried out by taking for each temperature T, the values of H_p at the first minimum, H_{on} at the first maximum, H_{sp} at the second minimum of the associated magnetization curves in Figs. 2–4, and transfer them to the corresponding points in Fig. 7. The data points for H_{irr} in the same figure are obtained, again for each T, from the corresponding points of splitting between the lower and upper branches of M-H curves in Figs. 2–4. This transformation of domain data allows a better description and a more convenient study of the temperature and field-dependent behaviors of the sample on the basis of available theoretical models, and thus paves the way for the construction of the associated phase diagram.

In Fig. 7, the data are presented together with the theoretical fits. One of the noticeable features in the H-T diagram is

the appearance of an apparently well-confined region for the peak effect, corresponding to the region containing the ''rising'' part of the magnetic response (or the descending part of the associated magnetization curve pertaining to the second peak). This region is limited on the left-hand and right-hand sides to 11 and 19.5 K, respectively, as alluded earlier. It is bounded below by the H_{on} curve corresponding to the onset fields of the second peak, and bounded above by the H_{sp} curve representing the fields at the peaks. In accordance with the order-disorder transition model for the peak effect,[11,12] H_{on} is supposed to represent the boundary for the transition from the vortex-lattice state to the vortex-glass state, which was recently suggested to be an entangled solid phase of the vortices.[13] It is important to point out, however, that in contrast to previous reports,[17,18] our data for H_{on} do not fully confirm the characteristic temperature dependency expressed by $H_{on}(T)=H_{on}(0)[1-(T/T_c)^4]^{3/2}$ as proposed by Giller *et al.*,[18] particularly for $T/T_c > 0.8$. Neither do we observe a dramactic rise of H_{on} at low temperature as reported by Andrade *et al.*[17] The upper boundary H_{sp} marks the turning point corresponding to the sharp reversal of the magnetic response of the sample, which is presumably a consequence of sudden weakening of the pinning strength. One potential mechanism responsible for this change of pinning effect at relatively high magnetic fields is a dimensional crossover from a 3D to a 2D vortex state. This 2D vortex state may exist below the vortex melting line $H_{irr}(T)$ as a result of pancake vortex-layer decoupling at relatively high fields. An estimate of the dimensional crossover field based on the approximate formula[20] $H_{2D}(0)\approx 4\Phi_0/(\gamma d)^2$ with anisotropy[16] $\gamma=200$, and interlayer spacing $d=12$ Å yields a value of about 1400 Oe for $H_{2D}(0)$ as indicated on the field axis in Fig. 7. The fact that this value of $H_{2D}(0)$ is closer to the value commonly cited for BSCCO than that for YBCO may well be related to its higher anisotropy compared to YBCO due to the absence of apical oxygen in NCCO. A straight line drawn from that point intersects the H_{sp} curves near its upper end, at $T\sim 11$ K, suggesting that our H_{sp} curve may signify the harbinger of a dimensional crossover in the higher-temperature region. It must be stressed that the boundary of dimensional crossover, which is commonly indicated by the straight horizontal line drawn from $H_{2D}(0)$, is strictly valid only in the low-temperature region far away from T_c. On a general ground, it is expected to curve down due to weakening of interlayer coupling at higher temperature, perhaps similar to the way H_{sp} decreases toward T_c. One notes further in that this so-called second-peak field H_{sp} exhibits a temperature dependence described very closely by $H_{sp}(T)=H_0(1-T/T_c)^{1.25}$, for $H_0=2650$ Oe, resembling the high-temperature part of H_{irr} to be discussed in the following. Unfortunately, to our knowledge, this interesting observation has so far remained unexplained.

It is important to note at this point that the H_{on} curve in Fig. 7 is located slightly above the penetration field curve H_p, supporting our view that the peak effect occurs in a state where effective penetration of the external field as well as the formation of quasilattice structure have taken place in the sample, and the pinning mechanism becomes operative. Further, an abrupt upward shift of H_p occurs at T around the lower limit of the temperature range of the second peak. In other words, effective formation of the vortex state in the sample will only take place at these higher magnetic fields below 10 K. It is then interesting to note that this lower-temperature part of the H_p curve is located above the $H_{2D}(0)$ line. This implies that such a strong increase in magnetic field will take the vortex right into the 2D regime where no lattice vortex structure can be supported[21] and hence no lattice-glass transition or second-peak effect is expected to occur. This explains quite naturally the disappearance of the second peak below 11 K. It is understood that H_p is mostly determined by barrier effects, and this effect is presumably enhanced at lower temperature, explaining the need of a higher external field for its effective penetration into the sample. Ignoring the relaxation effect, a surface-barrier model for pancake vortices[22] has been proposed to be characterized by $H_p\simeq H_c\exp(-T/T_0)$. As seen in Fig. 7, the low-temperature part of H_p fits very well with the data for $H_c=6800$ Oe and $T_0=6.2$ K. On the other hand, the higher-temperature part of H_p fits only partially with the theoretical curve (using $H_c^*=1000$ Oe), exhibiting distinct deviation at temperatures close to T_c. A vortex-line model with its prediction of $H_p\sim(T_c-T)^{3/2}/T$ does not work either for this part of the data.[23] We suspect that the additional effect of geometrical barriers may play a greater role at higher temperature.[24,25]

Turning our attention to the irreversibility line in Fig. 7, we note immediately that the data are clearly divided into two parts. The high-temperature part ($11\ \text{K}<T<19.5$ K) displays an excellent fit to the theoretical curve given by $H_{irr}=H_m(1-T/T_c)^{1.5}$ for $H_m=13\,500$ Oe, which was supposed to be a consequence of depinning of the vortices or the combined effect of thermal and quantum fluctuations.[26] We note once again that Andrade *et al.*[17] have reported a fit of their data with basically the same form for $H_m=23\,000$ Oe and an exponent of 2.4. One further observes that below 10 K, the irreversible line is better characterized by an exponential law, $H_{irr}=H_m^*\exp(b_0/T)$ where $H_m^*=2500$ Oe and $b_0=10$ K. This behavior has been suggested in the Josephson-coupled layer-superconductor model with moderate anisotropy.[27] A similar change of the temperature-dependent behavior of H_{irr} was also observed in a single crystal of BSCCO (Refs. 27, 4, and 28–30) and TBCO.[31] In contrast to that observation, however, the discontinuity found here involves the value of H_{irr} instead of merely its slope. Furthermore, a change in sign of the slope was observed at the onset temperature in the case of the BSCCO and TBCO system. In our case, this change cannot be observed since the onset temperature at the higher end is too close to T_c to allow such a detailed analysis. It is conceivable to expect, however, that some change in H_{irr} should occur at both ends of the temperature range of the peak effect. In our case, for instance, the discontinuity at lower temperature and higher magnetic field could perhaps be attributed to some change in the interlayer-coupling mechanism, while the change at temperatures close to T_c may well be due to fluctuation-induced depinning effects. It is nevertheless too early at this stage to pin down the exact nature of the changes. In fact the theoretical model mentioned above was formulated for a 3D-like vortex fluctuation at $H\ll H_{2D}(0)$, which is not exactly the condition met in our experiment. But the fact that it occurs concurrently with the onset or disappearance of the peak ef-

fect should provide an important clue for the unraveling of its underlying mechanism.

Finally, a note of comparison with the vortex-phase-transition picture proposed recently by Giller *et al.*[18] will be in order. We note in the first place that their H-T diagram does not indicate the existence of a low-temperature limit for the entangled solid phase as revealed by our experimental data and indicated in the vortex phase diagram. We should also point out that in our proposed phase diagram, a ''buffer'' vortex phase of 2D or quasi-2D character appears between the phase boundary of the entangled solid and the vortex melting line $H_{irr}(T)$. In addition to this, detailed temperature-dependent behavior of the various ''phase'' boundaries obtained from our data is also at variance with theirs.

CONCLUSION

We have presented magnetization data on a NCCO single crystal at various temperatures, which show a clear temperature delineation on both ends for the second-peak effect and an abrupt increase of the penetration field at its lower end. Analysis of the data on the basis of some of the existing models has led to a suggested vortex-state phase diagram for the sample. It also confirms the crucial role of pinning with weak disorder in the peak effect, and suggests the necessary condition of effective penetration by the external field along with the formation of a quasilattice vortex state, which is only possible in the 3D-vortex regime. Lacking any of these factors will simply lead to an unfavorable condition for the appearance of the peak effect. We have further found a compelling reason to include the quasi-2D vortex regime in our H-T diagram in order to understand the important characteristics of our data. Our H-T phase diagram also reveals a number of features in conjunction with the appearance of this anomalous effect, which requires a more comprehensive and coherent explanation. Finally, it is important to point out that our data do not agree very well with those obtained by the other groups on the same basic system, prepared, however, by different processes. This sample-dependent nature of the data is further demonstrated by our magnetization measurements on the same samples of different thicknesses, which will be reported elsewhere.

ACKNOWLEDGMENTS

We thank P. H. Kes for reading the manuscript as well as for comments and suggestions. We are grateful to FOM-ALMOS for the use of sample preparation and characterization facilities. We would also like to thank Ton Gortermulder for the help with EPMA analysis. This work was supported by Van der Waals–Zeeman Institute through KNAW under Project No. 95-BTM-33 and Jurusan Fisika ITB through RUT project under Contract No. 207/SP/RUT/BPPT/97.

[1] M. Daeumling, J. M. Seuntjen, and D. C. Larbalestier, Nature (London) **346**, 332 (1990).
[2] V. N. Kopylov, A. E. Koshelev, I. F. Schegolev, and T. G. Togonidze, Physica C **170**, 291 (1990).
[3] N. Chikumoto, M. Konczykowski, N. Motohira, and A. P. Malozemoff, Phys. Rev. Lett. **69**, 1260 (1992).
[4] K. Kadowaki and T. Mochiku, Physica C **195**, 247 (1992).
[5] T. Kimura, K. Kishio, T. Kobayashi, Y. Nakamura, N. Motohira, K. Kitazawa, and K. Yamafuji, Physica C **192**, 247 (1992).
[6] F. Zuo, S. Khizroev, Xiuguang Jiang, J. L. Peng, and R. L. Greene, Phys. Rev. B **49**, 12 326 (1994).
[7] L. Krusin-Elbaum, L. Civale, V. M. Vinokur, and F. Holtzberg, Phys. Rev. Lett. **69**, 2280 (1992).
[8] G. Yang, P. Shang, S. D. Sutton, I. P. Jones, J. S. Abell, and C. E. Gough, Phys. Rev. B **48**, 4054 (1993).
[9] T. Tamegai, Y. Iye, I. Ogura, and K. Kishio, Physica C **213**, 33 (1993).
[10] Y. Abulafia, A. Shaulov, Y. Wolfus, R. Prozorov, L. Burlachkov, Y. Yeshurun, D. Majer, E. Zeldov, H. Wühl, V. B. Geshkenbein, and V. M. Vinokur, Phys. Rev. Lett. **77**, 1596 (1996).
[11] T. Giamarchi and P. Le Doussal, Phys. Rev. B **55**, 6577 (1997).
[12] A. E. Koshelev and V. M. Vinokur, Phys. Rev. B **57**, 8026 (1998).
[13] V. Vinokur, B. Khaykovich, E. Zeldov, M. Konczykowski, R. A. Doyle, and P. H. Kes, Physica C **295**, 209 (1998).
[14] E. Zeldov, D. Majer, M. Konczykowski, A. I. Larkin, V. M. Vinokur, V. B. Geshkenbein, N. Chikumoto, and H. Shtrikman, Europhys. Lett. **30**, 367 (1995).
[15] C. D. Dewhurst, D. A. Cardwell, A. M. Campbell, R. A. Doyle, G. Balakrishnan, and D. McK. Paul, Phys. Rev. B **53**, 14 594 (1996).
[16] F. Zuo, S. Khizroev, X. Jiang, J. L. Peng, and R. L. Greene, Phys. Rev. Lett. **72**, 1746 (1994).
[17] M. C. de Andrade, N. R. Dilley, F. Ruess, and M. B. Maple, Phys. Rev. B **57**, R708 (1998).
[18] D. Giller, A. Shaulov, R. Prozorov, Y. Abulafia, Y. Wolfus, L. Burlachkov, Y. Yeshurun, E. Zeldov, V. M. Vinokur, J. L. Peng, and R. L. Greene, Phys. Rev. Lett. **79**, 2542 (1997).
[19] C. D. Dewhurst and R. A. Doyle, Phys. Rev. B **56**, 10 832 (1997).
[20] L. I. Glazman and A. E. Koshelev, Phys. Rev. B **43**, 2835 (1991).
[21] Cheng Zeng, P. L. Leath, and D. S. Fisher, Phys. Rev. Lett. **82**, 1935 (1999).
[22] L. Burlachkov, V. B. Geshkenbein, A. E. Koshelev, A. I. Larkin, and V. M. Vinokur, Phys. Rev. B **50**, 16 770 (1994).
[23] M. Niderost, R. Frassanito, M. Saalfrank, A. C. Mota, G. Blatter, V. N. Zavaritsky, T. W. Li, and P. H. Kes, Phys. Rev. Lett. **81**, 3231 (1998).
[24] D. Majer, E. Zeldov, and M. Konczykowski, Phys. Rev. Lett. **75**, 1166 (1995).
[25] R. A. Doyle, S. F. W. R. Rycroft, T. B. Doyle, E. Zeldov, T. Tamegai, and S. Ooi, Phys. Rev. B **58**, 135 (1998).
[26] Gianni Blatter and B. Ivlev, Phys. Rev. Lett. **70**, 2621 (1993).
[27] A. Schilling, R. Jin, J. D. Guo, and H. R. Ott, Phys. Rev. Lett. **71**, 1899 (1993).
[28] L. W. Lombardo, D. B. Mitzi, A. Kapitulnik, and A. Leone, Phys. Rev. B **46**, 5615 (1992).
[29] C. J. van der Beek and P. H. Kes, Phys. Rev. B **43**, 13 032 (1991).
[30] J. Yazyi, A. Arrbére, C. Durán, F. de la Cruz, D. B. Mitzi, and A. Kapitulnik, Physica C **184**, 254 (1991).
[31] F. Zuo, S. Khizroev, G. C. Alexandrakis, and V. N. Kopylov, Phys. Rev. B **52**, R755 (1995).